

Wigner Cat Phases: A finely tunable system for exploring the transition to quantum chaos

M. Süzen ^{a,b*}

^a Resident Scientist, Assia, CY 5561, Cyprus and

^b American Physical Society, Member, College Park, MD

(Dated: March 10, 2026)

A quantum mechanical setting consisting of a frozen qubit composed with a fully thermalized chaotic system of N states is proposed, with potential relevance to quantum control. Observing the states of the composed system selectively retaining the states leads to the observation of novel localization in the subsystem. At a tuning parameter of 1.0, implying no selection, the system exhibits Wigner-Dyson level spacing statistics, indicative of quantum chaos. As the tuning parameter is reduced and selection occurs at a cutoff, the nearest-neighbor level spacing distribution develops heavier tails, a signature of suppressed spectral mixing and the emergence of non-thermal dynamics. In these regimes, the eigendensity develops a pronounced "cat-ears" structure, reflecting the formation of spatially localized bimodal eigenstates. These topological features persist without transitioning to Poisson statistics, indicating a transition from quantum chaos to a non-thermal, novel many-body localized (MBL) regime—referred to as Wigner Cat Phases. The proposed mixed random matrix ensemble offers a practical probe for sustaining this novel quantum localization setting. Results from our rigorous spectral statistics analysis show how "cat-ears" form in spectral densities based on the degree of selection or disorder and indicate that gap ratio statistics must be used with caution in detecting the full integrable limit due to the possibility of heavy-tailed Wigner-Dyson distributions.

Keywords: quantum chaos, spectral fluctuations, random matrix theory, eigenstate thermalization, many-body localization, quantum control

I. INTRODUCTION

The correspondence between classical and quantum mechanical descriptions of systems exhibiting classical chaos has long fascinated physicists [1–5]. How to define and quantify quantum chaos remains a central topic [6–16]. Among these, the Bohigas-Giannoni-Schmit (BGS) conjecture [17] stands out as a foundational result: it predicts that quantum systems with classically chaotic dynamics exhibit level spacing statistics governed by Wigner-Dyson ensembles—specifically, invariant random matrix ensembles whose classical counterparts are chaotic and ergodic [18–31]. This connection is commonly referred to as quantum chaology (originally introduced by Sir Michael Berry [32]), though we use the term quantum chaos for consistency with the broader literature. In prior work, Sir Berry's conjecture [6, 33, 34] proposed that high-energy eigenstates are described by wavefunctions drawn from a Gaussian random ensemble of plane waves.

Researchers have identified connections between the BGS conjecture and the emergence of quantum ergodicity through random matrix theory, particularly via the Eigenstate Thermalization Hypothesis (ETH) [35–39], as reviewed in [40, 41] and recently extended using tools such as the Loschmidt echo and out-of-time-order correlators (OTOC) [42–44]. Recent work has highlighted parallels between ETH and BGS statistics [45], stimulating

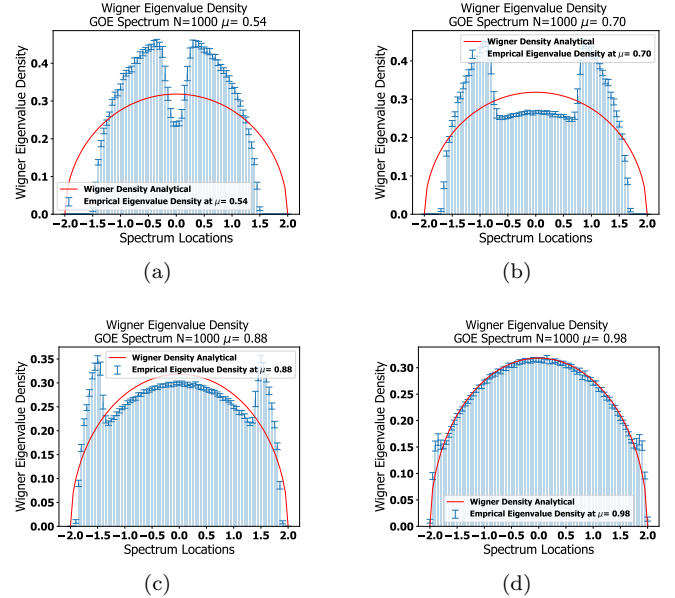


FIG. 1. Spectral densities are numerically computed for different tuning parameters, as shown in (1a) $\mu = 0.54$, (1b) $\mu = 0.70$, (1c) $\mu = 0.88$ and, (1d) $\mu = 0.98$. These are referred to as Wigner Cat Phases due to their M-shaped spectral densities, which deviate from Wigner's semicircle law. Uncertainties are estimated using bootstrapped 95% confidence intervals from the mGOE ensemble, and are displayed as error bars. We observe that the semicircle law is recovered at small mixing strengths, i.e., at higher values of μ .

* mehmet.suzen@physics.org

formation theory and its applications [46–52], especially in novel detection protocols [53].

A localization phenomenon in which full thermalization is not achieved—many-body localization (MBL) [54]—remains an active area of research. Key open questions include: how MBL phases emerge, and what their spectral and dynamical properties are from a random matrix theory perspective.

Recently, multi-parametric ensembles have been employed to describe non-ergodic regimes [55–60], leveraging local spectral and eigenfunction statistics. In contrast, we introduce a new class of invariant random matrix ensembles—a mixed Wigner-Dyson ensemble—distinct from the Brownian ensemble [58]. Our framework provides a continuous description of the transition to ergodicity within a single ensemble, characterized by an order parameter that reveals signatures of novel many-body localized phases.

II. WIGNER CAT PHASES: COMPOSITE SYSTEM WITH FROZEN QUBIT

Experimental realization of many-body localization (MBL) remains an active area of research, with systems such as superconducting qubits [61–63] representing key progress. In this context, our approach provides a diagnostic tool for identifying novel MBL phases. The construction of Wigner cat phases leverages selective state treatment—a concept rooted in foundational quantum mechanics, such as the Born-Oppenheimer approximation [64]. This principle inspires quantum control, a central challenge in scalable quantum information processing, as seen in recent studies of single magnon spins [65] and frozen nuclear spins [66], with implications for fault-tolerant quantum memory [67]. State freezing enables selective access to subspace dynamics, which may be exploited in quantum optimization algorithms [68], enhancing scalability through a restricted set of states. Such frozen coherence has also been explored in protected quantum states [69, 70]. Here, we implement selective treatment of a composite quantum system to realize Wigner cat phases, which are numerically accessible within a mixed random matrix ensemble.

A mixed ensemble of energy matrices is proposed by composing two systems: a frozen qubit and a thermalized secondary N -state quantum system that is chaotic. Composing multiple finite Hilbert spaces [71] or decomposing a single one [72] are active areas of research in the development of practical quantum processes. The composite system considered here consists of a frozen qubit and an N -state quantum chaotic system.

Considering these two quantum systems mathematically yields to composition of two Hilbert Spaces, $\mathcal{H}_1 \cong \mathbb{C}^2$ and $\mathcal{H}_2 \cong \mathbb{C}^N$, where \cong denotes isomorphic equivalence. The composite system is given by [72],

$$\mathcal{H} = \mathcal{H}_1 \otimes \mathcal{H}_2. \quad (1)$$

We can write total energy operators in matrix form, $H_1 \in \mathbb{C}^{2 \times 2}$ and $H_2 \in \mathbb{C}^{N \times N}$, for frozen qubit and for fully thermalized system attaining quantum chaos respectively. Here, \times denotes matrix multiplication (i.e., the tensor product), consistent with the dimensions of vectors in the Hilbert space. Then, the total energy of the composed system is given by [72],

$$H = \mathbb{I}_N \otimes H_1 + \mathbb{I}_2 \otimes H_2 + H_{int}, \quad (2)$$

where $\mathbb{I}_2 \in \mathbb{C}^{2 \times 2}$ and $\mathbb{I}_N \in \mathbb{C}^{N \times N}$ are identity matrices, and H_{int} is the interaction energy matrix.

In the case of a frozen qubit, $H_1 = 0$ and $H_{int} = 0$. Then, the composed system, described by the total energy H , becomes,

$$H = \mathbb{I}_2 \otimes H_2 = \begin{pmatrix} H_2 & \mathbf{0} \\ \mathbf{0} & H_2 \end{pmatrix}, \quad (3)$$

where $\mathbf{0} \in \mathbb{C}^{N \times N}$ is the zero matrix.

As H_2 represents quantum chaotic system or in thermalized state, due to BGS conjecture [17], we can model H_2 as a random matrix from Wigner-Dyson family, Gaussian Orthogonal Ensemble (GOE). Then the spectrum of composite energy H and its component H_2 are given by,

$$\sigma(H_2) = \{\lambda_1, \dots, \lambda_N\}, \quad (4)$$

$$\sigma(H) = \{\lambda_1, \dots, \lambda_N, \lambda_1, \dots, \lambda_N\}. \quad (5)$$

We conjecture that restricting the spectrum of H by truncating the eigenvalues at a given fraction—preserving the ordering of the energy levels—we retain the first μ percent of the eigenenergies, corresponding to a subsystem of the composite system. Here, μ acts as a mixing or effective coupling parameter, interpolating between fully delocalize and partially localized regimes. At $\mu = 1.0$, the system exhibits fully developed quantum chaos, consistent with the Wigner-Dyson level statistics of the full spectrum. As μ is decreased, a novel localization regime emerges—referred to as Wigner cat phases—where the empirical spectral density displays a characteristic “cat-ear” structure: a bimodal peak with two distinct, spatially separated energy clusters. This behavior arises from the formation of spatially localized bimodal eigenstates, which are non-orthogonal and exhibit a wavefunction structure resembling a superposition of two distinct classical states (analogous to a Schrödinger cat state). Although the full system remains quantum chaotic, the truncated spectrum effectively suppresses dynamical interactions across the full Hilbert space, leading to the emergence of these non-ergodic, structured eigenstates. Importantly, this transition is not a breakdown of quantum chaos, but rather a manifestation of ergodicity breaking under spectral truncation—a phenomenon reminiscent of many-body localization (MBL) in non-interacting systems, though here the localization

is driven by spectral selection rather than induced disorder.

Using a numerical procedure that mimics the spectral properties of this physical setting is possible via considering different size matrices and repeated eigenvalues with periodic boundary conditions in spectra, mixed GOE (mGOE). *This is essentially finding eigenvalues of H_2 first and then extending the known ones up to μ ratio, due to the symmetry in H .* We achieved an enhanced statistical uncertainty by using a Binomial distribution to generate different size matrices at a given mixture parameter.

The equivalent construction of this physical setting as a numerical procedure is possible by considering different-size matrices for H_2 , with eigenvalues sampled from the GOE. Spectra from matrices of different sizes are aligned up to a total number of states N through cyclic extension up to a cutoff. This procedure is analogous to applying periodic boundary conditions in the truncated spectrum. Due to the translational symmetry of H , eigenvalues of H_2 can be systematically extended across matrix sizes, allowing known eigenvalues to be propagated to the μ ratio. Furthermore, improved sampling is achieved by using a binomial distribution to generate matrices of varying sizes at a fixed mixture parameter.

III. NUMERICAL CONSTRUCTION OF MIXED ENSEMBLE

The primary invariant ensemble that represents a quantum chaotic system, as proposed by the BGS conjecture, is the Gaussian Orthogonal Ensemble (GOE). Its numerical construction was clearly demonstrated in the seminal work of *Edelman–Rao* [73], among other generalized ensembles. Here, we focus on the GOE. A given matrix G_1 with entries drawn from a Gaussian distribution with mean 0 and standard deviation σ can be used to sample a member of the GOE ensemble $A^{GOE}(N)$ via the following algebraic equality [73]:

$$A^{GOE}(N) = \frac{1}{2}(G_1(N) + G_1^T(N)), \quad (6)$$

where $G_1^T(N)$ denotes the transpose of $G_1(N)$. The sampled matrix $A^{GOE}(N)$ has the following properties:

1. Diagonal elements follow a normal distribution with variance σ : $diag(A^{GOE}) \sim \mathcal{N}(0, \sigma)$,
2. Off-diagonal elements follow a normal distribution variance $\sigma/2$: $offdiag(A^{GOE}) \sim \mathcal{N}(0, \sigma/2)$.

If we draw M random matrices, the resulting ensemble of size M with square matrix dimensions N is denoted $GOE(M, N)$. This construction allows us to estimate bootstrapped confidence intervals for all computed observables [74, 75]. While such confidence intervals are

not commonly employed in standard random matrix theory (RMT) studies, they become particularly important in our context—especially for mixed ensembles—due to the numerical nature of their generation and the inherent finite-sample fluctuations in the ensemble construction.

A mixed ensemble is constructed by varying the matrix sizes within a sample of size M . We denote such a mixed Gaussian Orthogonal Ensemble (GOE) by $mGOE$, characterized by an additional parameter—the degree of mixture μ . The ensemble $mGOE(M, N, \mu)$ thus generalizes the standard $GOE(M, N)$ by allowing for a controlled distribution of matrix dimensions. In the limit $\mu \rightarrow 1.0$, the mixed ensemble reduces to the conventional GOE, such that $GOE(M, N) = \lim_{\mu \rightarrow 1.0} mGOE(M, N, \mu)$.

The numerical construction of the mixed ensemble $mGOE$ —or any mixed ensemble of a canonical random matrix ensemble—follows the following procedure:

1. We generate M random matrices, each of size n_i , drawn independently from the Gaussian Orthogonal Ensemble (GOE) of dimension n_i .
2. The number of matrices of size n_i is denoted by m_i , with the constraint $\sum_i m_i = M$.
3. The degree of mixture μ is interpreted as the success probability in a Bernoulli process, where each matrix size n_i is selected with probability proportional to μ , and the total count m_i follows a binomial distribution. In the limit $\mu \rightarrow 1.0$, the assignment of matrix sizes becomes deterministic and each matrix is assigned the same size N , recovering the standard GOE ensemble exactly.
4. The sequence of matrix sizes $\{n_i\}$ is generated through M independent Bernoulli trials with success probability μ and a fixed matrix dimension N , following a binomial distribution: $\text{Binomial}(\mu, N)$ —note that this refers to the distribution of the *number of matrices of a given size*, not the size itself. The actual size n_i is drawn from a discrete distribution over $n = 1, 2, \dots, N$, with probability proportional to μ .
5. The full set of M matrices is then drawn independently from $GOE(n_i)$, with the size n_i determined by the binomial process described above.
6. In the large- M limit, the ensemble average size satisfies the consistency condition $N\mu = \frac{1}{M} \sum_i m_i n_i$, which ensures that the average matrix size converges to N in the limit of large M and fixed μ .

IV. DETECTING LOCALIZATION TO EIGENSTATE THERMALIZATION

Progress has been made in studying the transition from integrability to non-integrability, a regime where the Eigenstate Thermalization Hypothesis (ETH)

is expected to emerge, both analytically and through parametrized approaches to spin models [54, 76–80]. From the perspective of the BGS conjecture, an interpolation between Poisson and Gaussian Orthogonal Ensemble (GOE) statistics in the distribution of consecutive level spacings appears prominently [78].

Here, we briefly review the canonical approach to detecting localization and quantum chaos through spectral statistics, and how the Eigenstate Thermalization Hypothesis (ETH) is formulated. A definite quantum state $|\Psi(t)\rangle$ evolves in time according to its eigenstates $|\alpha\rangle$ and eigenenergies E_α , with a time-dependent phase factor, via the expression:

$$|\Psi(t)\rangle = \sum_{\alpha} C_{\alpha} \exp(-iE_{\alpha}t)|\alpha\rangle, \quad (7)$$

where $\sum_{\alpha} |C_{\alpha}|^2 = 1$, ensuring normalization of the state. The emergence of thermal equilibrium — characterized by the time-averaged value of an observable A converging to a temperature-dependent value $\langle A \rangle_T$ — is described by two key conditions of the ETH [35–39]:

1. The diagonal matrix element $\langle \alpha | A | \alpha \rangle$ is a smooth function of the eigenenergy E_{α} , denoted $\Phi(E_{\alpha})$. This implies that individual energy eigenstates exhibit thermal behavior, with $\langle A \rangle_T = \Phi(E_{\alpha})$, independent of the initial state preparation.
2. For transitions between eigenstates α and β , the off-diagonal matrix element $\langle \alpha | A | \beta \rangle$ is exponentially suppressed compared to the diagonal elements, ensuring that thermalization arises from the properties of individual eigenstates.

This is also connected to quantum ergodicity, as the ensemble average $\langle A \rangle$ equals the time average of the observable A when thermalization is achieved. This profound and insightful characterization of quantum thermalization, originally established by Deutsch and Srednicki, provides a foundation for demonstrating that quantum systems whose classical counterparts exhibit chaotic behavior in the Lyapunov sense satisfy the two conditions of the Eigenstate Thermalization Hypothesis (ETH).

If we invoke the BGS conjecture, recent work has shown that its statistical predictions exhibit stronger consistency and predictive power due to its inherent statistical nature [45]. In this framework, Dyson–Wigner random matrices belonging to the Gaussian Orthogonal Ensemble (GOE) satisfy the thermalization hypothesis and are widely used to model quantum chaotic systems. We focus on this aspect: quantum chaotic systems are expected to reach thermal equilibrium under the assumptions of the eigenstate thermalization hypothesis (ETH). Deviations from such behavior signal the absence of thermalization, a phenomenon known as Many-Body Localization* (MBL). A more comprehensive theoretical treatment of MBL has recently been presented by Sierant–Lewenstein et al. [54] and references therein.

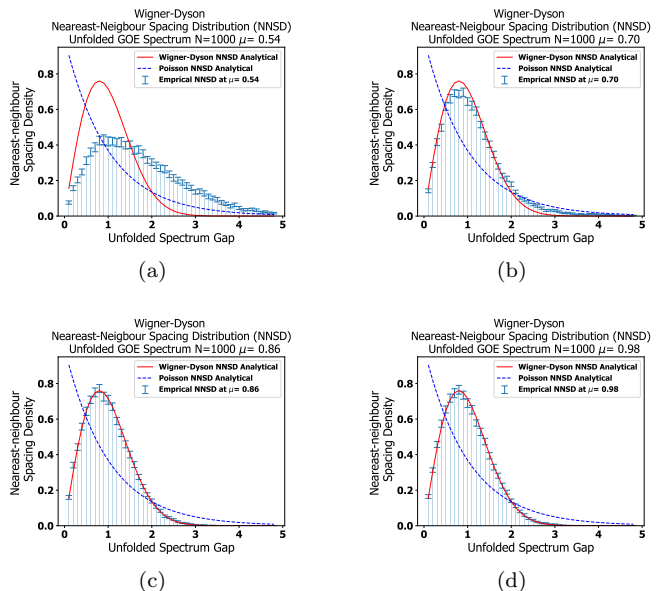


FIG. 2. Nearest-neighbor spacing distributions for different values of μ are shown: (2a) $\mu = 0.54$, (2b) $\mu = 0.70$, (2c) $\mu = 0.86$, and (2d) $\mu = 0.98$. For smaller μ , the distribution deviates from the Wigner-Dyson ensemble, with lower values indicating a heavy-tailed (Poisson-like) spectrum. Notably, full integrability is not observed at any value of μ , as the Poisson distribution is absent in all cases. The deviations from the Wigner-Dyson distribution at small μ are quantified using bootstrapped 95% confidence intervals, which are displayed as error bars. As μ increases, the spacing distribution approaches the Wigner-Dyson form, indicating the onset of quantum chaos and level statistics typical of chaotic systems.

The core problem reduces to the statistical identification of deviations from quantum chaos, under which conditions and in which systems such deviations occur. A prominent measure in this direction was introduced by Oganesyan–Huse in a seminal work [81], who investigated the many-body localization (MBL) transition through the analysis of adjacent gap ratios in the energy spectrum. Given N spectral spacings δ_i , after sorting the eigenenergies, the mean adjacent gap ratio r is computed as follows:

$$r = \frac{1}{N} \sum_{i=2}^N \frac{\min(\delta_i, \delta_{i-1})}{\max(\delta_i, \delta_{i-1})}. \quad (8)$$

They found that r takes values of 0.3860 and 0.5295, corresponding to full localization and full thermalization, respectively. These transition points are associated with Poisson and Wigner–Dyson distributed energy spectra, which characterize integrable and chaotic quantum systems, respectively. Our tunable ensemble, as described in the next section, can simulate this transition from eigenstate thermalization (ETH) to MBL phases. This phenomenon corresponds to a transition from quantum

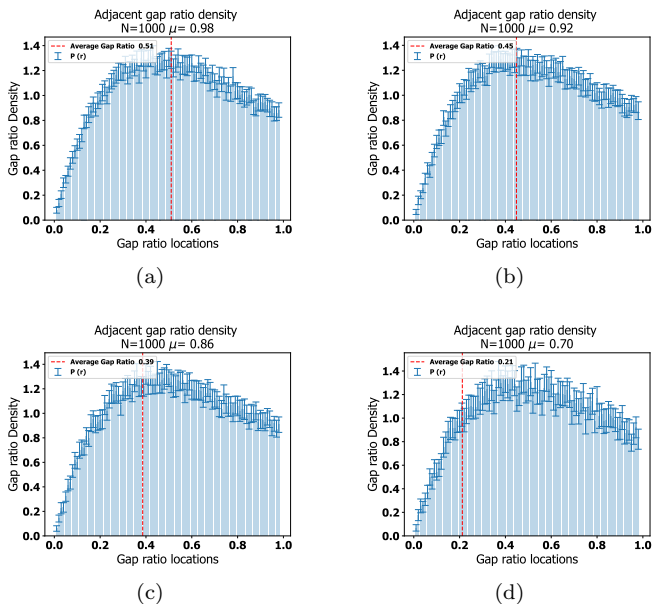


FIG. 3. Density of adjacent gap ratios with mean values marked at different degrees of mixing, (3a) $\mu = 0.98$, (3b) $\mu = 0.92$, (3c) $\mu = 0.86$, and (3d) $\mu = 0.70$. Uncertainties are computed over the mGOE ensemble via bootstrapped 95% confidence intervals and are displayed as error bars. We observe that the tail of the distribution changes at higher mixtures, i.e., for lower values of μ

integrability to non-integrability, and from quantum non-ergodicity to ergodicity.

A. Spectral Periodicity: Degeneracy and inducing localization

We establish a principled method for defining spectral densities. One such ensemble, the mixed Gaussian Orthogonal Ensemble (mGOE), naturally captures transitions to the eigenstate thermalization (ETH) regime and many-body localization (MBL) phases. Numerical simulations reveal so-called Wigner cat phases, characterized by M-shaped empirical spectral densities—offering a novel, topological fingerprint of many-body dynamics.

The procedure for generating mixed ensembles produces a variety of spectral densities with different matrix sizes. To enable meaningful comparison, we align the spectra by applying periodic boundary conditions. For a matrix of size n_i , the resulting spectrum consists of n_i eigenvalues. Periodicity enforces the repetition of these eigenvalues up to a base size N , consistent with the ensemble parameters $mGOE(N, M, \mu)$. This leads to level degeneracies in the energy spectrum.

In the study of localization phenomena, such as MBL, the degree of mixing μ serves as a tunable parameter that controls the transition between thermal and non-thermal phases. As μ increases, the system approaches full mix-

ing, corresponding to the ETH regime. Conversely, for $\mu < 1$, the system exhibits signatures of localization, with degeneracies and randomness arising from the binomial sampling process used to construct the mixed ensemble. This behavior is interpreted as a transition from delocalized to localized eigenstates.

The theoretical justification for this behavior lies in the mismatch between spectral analyses across different matrix sizes. This can be understood through the average behavior of the resulting spectral densities. The resulting spectral density exhibits a defect—a non-smooth, structured irregularity—due to the finite-size effects and spectral periodicity inherent in the ensemble. This defect is not a finite-size artifact but rather a conjectured intrinsic property of the mixed ensemble structure.

From a physical perspective, this defect can be interpreted as an induced disorder in the generation of the mixed ensemble, amplified by the spectral periodicity and the variation in matrix size. This mechanism mimics the spectral structure of the composite Hamiltonian introduced earlier in Equation 5, where the mixing of independent components leads to a structured, non-trivial energy spectrum.

B. Self-consistent spectral unfolding

Spectral unfolding is employed to remove local fluctuations and achieve locally flat spectra on average, facilitating a more reliable analysis of level statistics. As noted in the literature, the computation of nearest-neighbor spacing distributions can be sensitive to outliers in individual eigenvalues [82]. To mitigate this effect, we apply the interquartile range (IQR) of the eigenvalues for unfolding, ensuring that the resulting spectral distribution preserves the overall shape and statistical fidelity of the underlying ensemble. In the fully thermalized GOE regime, the unfolded spectrum exhibits perfect agreement with the theoretical prediction of a flat, locally uniform spacing distribution — confirming the effectiveness of this procedure in preserving the correct spectral statistics.

A self-consistent procedure is implemented by considering multiple polynomial fits of a given degree and selecting the degree that minimizes the mean fluctuation of the unfolded spacings, with the goal of achieving a distribution where the mean deviation from unity is minimized. Although the adjacent gap ratio distribution is inherently robust to unfolding, we adopt the unfolded spectrum for all subsequent spectral analyses to ensure consistency.

The evolution of the nearest-neighbor spacing distribution (NNSD) with varying mixture parameters is numerically identified. Spectral computations are performed using self-consistent unfolding and the truncation of spectral outliers [82, 83]. The ratio of consecutive level spacings (adjacent gap ratio) is also analyzed across a continuous transition, which is accessible within the mixed Gaussian orthogonal ensemble (mGOE) frame-

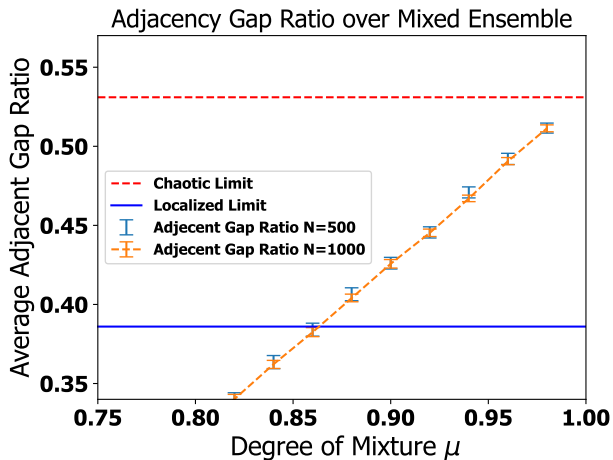


FIG. 4. Average (mean) gap ratios as a function of mixture strength μ reveal the evolution of localization properties. The horizontal lines indicate the transition points: one corresponds to full eigenstate thermalization (ETH), characterized by a gap ratio distribution approaching the Wigner-Dyson (GOE) prediction, while the other marks full integrability, where the ratio distribution follows Poisson statistics. However, in our system, despite the r ratio, we don’t observe Poisson distribution due to heavy-tails.

work. These transitions correspond to distinct regimes of localization strength and the emergence of different many-body localized (MBL) phases. As established in the literature, the adjacent gap ratio is a preferred quantity for such analyses due to its insensitivity to spectral unfolding procedures [78, 81, 84]. The continuous dependence of the mixture parameter enables finely resolved sampling from the mGOE, providing unprecedented resolution in the exploration of this novel MBL phase.

V. RIGOROUS SPECTRAL STATISTICS

A numerical investigation is conducted to examine how tuning the mixed Gaussian orthogonal ensemble (mGOE) parameter leads to a deviation from the limiting value $\mu = 1.0$. At this value, the eigenvalue statistics are consistent with the predictions of the eigenstate thermalization hypothesis (ETH), corresponding to the dynamics of a representative quantum system in the ergodic regime. A decrease in μ signifies a transition toward more localized eigenstates, indicative of the many-body localized (MBL) phase. Matrix sizes of $N = 1000$ and $N = 500$ are employed, with an ensemble sample size of $M = 100$, to quantify statistical uncertainties and assess the reliability of the observed transitions.

A dataset is generated using the mGOE framework at varying values of μ , with fixed ensemble size, to represent a quantum system undergoing a transition toward the MBL phase. To support this transition, we analyze the evolution of spectral and nearest-neighbor spacing

statistics, as well as the density of adjacent gap ratios, as functions of the tuning parameter μ . Additionally, we track the mean adjacent gap ratio across the tuning range to identify the values of μ for which the computed statistics converge to the expected behavior of full ETH and non-chaotic dynamics.

A. Wigner Cat Phases: Spectral Densities

Spectral densities are numerically identified for different tuning parameters, as shown in Figures 1a–1d for $\mu = 0.54, 0.70, 0.88, 0.98$, respectively. These are known as Wigner cat phases due to their M-shaped density profiles (“cat ears”), which deviate from Wigner’s semi-circular law. Uncertainties are computed over the mGOE ensemble using bootstrapped 95% confidence intervals, which are displayed as error bars. Some error bars are asymmetric, as there is no assumed distribution of the underlying errors. We observe that the semi-circular law is recovered at small mixtures, i.e., higher μ values.

As decreasing μ corresponds to increasing localization, the Wigner cat phases become more prominent, with the “cat ears” approaching closer together. We identify that this phenomenon arises from the interplay between eigenstate degeneracy and randomness, producing an effective defect structure, as discussed in the formulation of the mGOE generation procedure.

B. Spectral Nearest-Neighbor Spacings

Nearest-neighbor spacing statistics for different μ values are shown in Figures 2a–2d for $\mu = 0.54, 0.70, 0.86, 0.98$, respectively. Deviations from the Wigner-Dyson distribution are observed at smaller μ , with lower μ values exhibiting heavy-tailed spacing distributions. Uncertainties are computed over the mGOE ensemble using bootstrapped 95% confidence intervals, which are displayed as error bars. We observe that the Wigner-Dyson distribution is recovered at larger mixtures, i.e., higher μ values. These results support the possibility of many-body localized (MBL) phases characterized by heavy-tailed nearest-neighbor spacings. Notably, we do not observe a full Poissonian distribution even at small μ , indicating that the system does not exhibit integrable behavior. This suggests that the mGOE ensemble describes systems that can be tuned across a range of phases—from heavy-tailed localization to quantum chaos—manifesting a spectrum of non-thermal regimes, including the Wigner cat phases.

C. Transitions to quantum chaos: Adjacent Gap Ratios

We computed both mean values and distribution of adjacent gap ratios based on the Oganesyán–Huse mea-

sure. A key advantage of this quantity is that it does not require spectral unfolding, as it is insensitive to the unfolding procedure.

Density distributions of adjacent gap ratios, with mean values indicated at different values of the mixing parameter μ , are shown in Figures 3a–3d for $\mu = 0.98, 0.92, 0.86, 0.70$, respectively. Uncertainties are computed using bootstrapped 95% confidence intervals.

The mean values of the gap ratios provide insight into the degree of localization in the quantum dynamics. Varying the mixing strength μ describes the transition from quantum chaos to many-body localization. The mGOE ensemble naturally captures this transition in a continuous, linear fashion—this is quantified in Figure IV B.

We observe that in the localized limit—where the classical analog typically exhibits integrable behavior—the mGOE at this limit still exhibits non-integrable dynamics, as illustrated in Figure 3a. This behavior implies the emergence of a new many-body localized (MBL) phase that diverges from the conventional interpretation of the gap-ratio measure.

VI. CONCLUSION

We propose a composed quantum system featuring a frozen qubit that exhibits a novel form of localization when a subset of the spectrum is observed. This localization is tunable via the order parameter μ , which determines the cutoff in the partial observation of the spectral spectrum. Our extensive simulations are enabled by a

mixed Gaussian orthogonal ensemble (mGOE), which effectively models the composed system and benefits from enhanced statistical averaging.

Although the full composite system remains thermalized, a distinct form of localization emerges in the observed subsystem. Such selective spectral probing—where only a portion of the spectrum is monitored—opens the possibility for scalable quantum information processing. Furthermore, we demonstrate that many-body localized (MBL) phases with heavy-tailed nearest-neighbor spacings can exist, while still maintaining a mean adjacency gap consistent with an integrable system. This observation highlights the limitations of standard gap-ratio statistics in characterizing non-trivial MBL phases.

Data: The software toolkit Leymosun [85] is publicly available and enables reproducibility of the results, while the associated dataset is also accessible to the community [86].

Acknowledgments: We are grateful to Y. Süzen for her generous support of the *quantum dynamics* project. In particular, we thank her for encouraging the open release of the computational work as the freely available Python package Leymosun [85], designed for educational and pedagogical use, as well as for her valuable suggestions on how to present the material in an accessible and pedagogically effective manner. We also thank Dr. cand. Devanshu Shekhar from the Indian Institute of Technology, Kharagpur, and the broader quantum chaos community for their insightful comments and constructive feedback.

-
- [1] M. V. Berry, *New Scientist* **19**, 44 (1987).
 - [2] J. M. Martinis, M. H. Devoret, and J. Clarke, *Phys. Rev. B* **35**, 4682 (1987).
 - [3] J. Ford and G. Mantica, *American Journal of Physics* **60**, 1086 (1992).
 - [4] M. C. Gutzwiller, *Scientific American* **266**, 78 (1992).
 - [5] E. J. Heller and S. Tomsovic, *Physics Today* **46**, 38 (1993).
 - [6] M. V. Berry, *Journal of Physics A: Mathematical and General* **10**, 2083 (1977).
 - [7] B. Chirikov, F. Izrailev, and D. Shepelyansky, *Physica D: Nonlinear Phenomena* **33**, 77 (1988).
 - [8] W. H. Zurek and J. P. Paz, *Physica D: Nonlinear Phenomena* **83**, 300 (1995).
 - [9] K. Nakamura, *Quantum chaos: a new paradigm of nonlinear dynamics*, Vol. 3 (CUP Archive, 1994).
 - [10] B. Chirikov and G. Casati, *Quantum Chaos: Between Order and Disorder* (Cambridge University Press, 1995).
 - [11] H.-J. Stöckmann, *Quantum Chaos: An Introduction* (Cambridge University Press, 2009).
 - [12] A. Gubin and L. F. Santos, *American Journal of Physics* **80**, 246 (2012).
 - [13] M. C. Gutzwiller, *Chaos in Classical and Quantum Mechanics* (Springer Science & Business Media, 2013).
 - [14] S. Wimberger, *Nonlinear dynamics and quantum chaos*, Vol. 10 (Springer, 2014).
 - [15] F. Haake, S. Gnutzmann, and M. Kuś, *Quantum Signatures of Chaos*, 4th ed. (Springer Cham, 2018).
 - [16] E. J. Heller, *The semiclassical way to dynamics and spectroscopy* (Princeton University Press, 2018).
 - [17] O. Bohigas, M.-J. Giannoni, and C. Schmit, *Physical Review Letters* **52**, 1 (1984).
 - [18] J. Wishart, *Biometrika* **20**, 32 (1928).
 - [19] E. P. Wigner, *Mathematical Proceedings of the Cambridge Philosophical Society* **47**, 790 (1951).
 - [20] E. P. Wigner, *Annals of Mathematics* **62**, 548 (1955).
 - [21] E. P. Wigner, *Annals of Mathematics* **65**, 203 (1957).
 - [22] E. P. Wigner, *Annals of Mathematics* **67**, 325 (1958).
 - [23] E. P. Wigner, *SIAM Review* **9**, 1 (1967).
 - [24] F. J. Dyson, *Journal of Mathematical Physics* **3**, 1199 (1962).
 - [25] F. J. Dyson, *Journal of Mathematical Physics* **3**, 157 (1962).
 - [26] F. J. Dyson, *Journal of Mathematical Physics* **3**, 166 (1962).
 - [27] F. J. Dyson and M. L. Mehta, *Journal of Mathematical Physics* **4**, 701 (1963).
 - [28] M. L. Mehta and F. J. Dyson, *Journal of Mathematical*

- Physics **4**, 713 (1963).
- [29] M. L. Mehta, *Random Matrices*, 3rd ed., Vol. 142 (Elsevier, 2004).
- [30] T. Tao, *Topics in Random Matrix Theory*, Vol. 132 (American Mathematical Society, 2012).
- [31] M. Potters and J.-P. Bouchaud, *A first course in random matrix theory* (Cambridge University Press, 2020).
- [32] M. Berry, *Physica Scripta* **40**, 335 (1989).
- [33] M. V. Berry, in *Hamiltonian Dynamical Systems* (CRC Press, 2020) pp. 27–53.
- [34] C. Jarzynski, *Physical Review E* **56**, 2254 (1997).
- [35] J. M. Deutsch, *Phys. Rev. A* **43**, 2046 (1991).
- [36] M. Srednicki, *Physical Review E* **50**, 888 (1994).
- [37] M. Srednicki, *Annals of the New York Academy of Sciences* **755**, 757 (1995).
- [38] M. Srednicki, *Journal of Physics A: Mathematical and General* **29**, L75 (1996).
- [39] M. Srednicki, *Journal of Physics A: Mathematical and General* **32**, 1163 (1999).
- [40] L. D'Alessio, Y. Kafri, A. Polkovnikov, and M. Rigol, *Advances in Physics* **65**, 239 (2016).
- [41] J. M. Deutsch, *Reports on Progress in Physics* **81**, 082001 (2018).
- [42] L. Foini and J. Kurchan, *Phys. Rev. E* **99**, 042139 (2019).
- [43] S. Pappalardi, L. Foini, and J. Kurchan, *Phys. Rev. Lett.* **129**, 170603 (2022).
- [44] L. Foini, A. Dymarsky, and S. Pappalardi, *SciPost Phys.* **18**, 136 (2025).
- [45] H. A. Weidenmüller, *Journal of Physics A: Mathematical and Theoretical* **58**, 385003 (2025).
- [46] J. Cotler, N. Hunter-Jones, J. Liu, and B. Yoshida, *Journal of High Energy Physics*, 48 (2017).
- [47] J. M. Magán, *Journal of High Energy Physics* **2018**, 43 (2018).
- [48] T. Ali, A. Bhattacharyya, S. S. Haque, E. H. Kim, N. Moynihan, and J. Murugan, *Phys. Rev. D* **101**, 026021 (2020).
- [49] A. Altland, K. W. Kim, T. Micklitz, M. Rezaei, J. Sonner, and J. J. M. Verbaarschot, *Phys. Rev. Res.* **6**, 033286 (2024).
- [50] S.-D. Börner, C. Berke, D. P. DiVincenzo, S. Trebst, and A. Altland, *Phys. Rev. Res.* **6**, 033128 (2024).
- [51] A. Anand, S. Srivastava, S. Gangopadhyay, and S. Ghose, *Scientific Reports* **14**, 26890 (2024).
- [52] Google Quantum AI Team, *Nature* **646**, 825 (2025).
- [53] A. K. Das, C. Cianci, D. G. A. Cabral, D. A. Zarate-Herrada, P. Pinney, S. Pilatowsky-Cameo, A. S. Matsoukas-Roubeas, V. S. Batista, A. del Campo, E. J. Torres-Herrera, and L. F. Santos, *Phys. Rev. Res.* **7**, 013181 (2025).
- [54] P. Sierant, M. Lewenstein, A. Scardicchio, L. Vidmar, and J. Zakrzewski, *Reports on Progress in Physics* **88**, 026502 (2025).
- [55] W. Buijsman, V. Cheianov, and V. Gritsev, *Phys. Rev. Lett.* **122**, 180601 (2019).
- [56] W.-J. Rao, *Physica A: Statistical Mechanics and its Applications* **590**, 126689 (2022).
- [57] W. Rao, F. Zhao, and Y. Wang, *The European Physical Journal Plus* **139**, 722 (2024).
- [58] D. Shekhar and P. Shukla, *Journal of Physics A: Mathematical and Theoretical* **56**, 265303 (2023).
- [59] D. Shekhar and P. Shukla, *Phys. Rev. E* **112**, 024122 (2025).
- [60] D. Shekhar and P. Shukla, *Phys. Rev. E* **112**, 024123 (2025).
- [61] K. Xu, J.-J. Chen, Y. Zeng, Y.-R. Zhang, C. Song, W. Liu, Q. Guo, P. Zhang, D. Xu, H. Deng, K. Huang, H. Wang, X. Zhu, D. Zheng, and H. Fan, *Phys. Rev. Lett.* **120**, 050507 (2018).
- [62] Q. Guo, C. Cheng, Z.-H. Sun, Z. Song, H. Li, Z. Wang, W. Ren, H. Dong, D. Zheng, Y.-R. Zhang, R. Mondaini, H. Fan, and H. Wang, *Nature Physics* **17**, 234 (2021).
- [63] Z.-H. Liu and et al., *Nature* **650**, 79 (2026).
- [64] M. Born and R. Oppenheimer, *Annalen der Physik* **389**, 457 (1927).
- [65] D. Xu, X.-K. Gu, H.-K. Li, Y.-C. Weng, Y.-P. Wang, J. Li, H. Wang, S.-Y. Zhu, and J. Q. You, *Phys. Rev. Lett.* **130**, 193603 (2023).
- [66] M. T. Madzik, T. D. Ladd, F. E. Hudson, K. M. Itoh, A. M. Jakob, B. C. Johnson, J. C. McCallum, D. N. Jamieson, A. S. Dzurak, A. Laucht, and A. Morello, *Science Advances* **6**, eaba3442 (2020).
- [67] S. Bravyi, A. W. Cross, J. M. Gambetta, D. Maslov, P. Rall, and T. J. Yoder, *Nature* **627**, 778 (2024).
- [68] R. Ayanzadeh, N. Alavisamani, P. Das, and M. Qureshi, in *Proceedings of the 28th ACM International Conference on Architectural Support for Programming Languages and Operating Systems, Volume 2*, ASPLOS 2023 (Association for Computing Machinery, New York, NY, USA, 2023) p. 311–324.
- [69] T. R. Bromley, M. Cianciaruso, and G. Adesso, *Phys. Rev. Lett.* **114**, 210401 (2015).
- [70] Y. Fu, W. Liu, Y. Wang, C.-K. Duan, B. Zhang, Y. Wang, and X. Rong, *Phys. Rev. Appl.* **22**, 054067 (2024).
- [71] M. A. Nielsen and I. L. Chuang, *Quantum computation and quantum information* (Cambridge University Press, 2010).
- [72] S. M. Carroll and A. Singh, *Phys. Rev. A* **103**, 022213 (2021).
- [73] A. Edelman and N. R. Rao, *Acta Numerica* **14**, 233 (2005).
- [74] R. J. Tibshirani and B. Efron, **57**, 1 (1993).
- [75] A. C. Davison and D. V. Hinkley, *Bootstrap methods and their application*, 1 (Cambridge University Press, 1997).
- [76] M. V. Berry and M. Robnik, *Journal of Physics A: Mathematical and General* **17**, 2413 (1984).
- [77] L. F. Santos, *Journal of Physics A: Mathematical and General* **37**, 4723 (2004).
- [78] N. Chavda, H. Deota, and V. Kota, *Physics Letters A* **378**, 3012 (2014).
- [79] P. Sierant and J. Zakrzewski, *Phys. Rev. B* **99**, 104205 (2019).
- [80] S. Pai, N. Srivatsa, and A. E. Nielsen, *Physical Review B* **102**, 035117 (2020).
- [81] V. Oganesyan and D. A. Huse, *Phys. Rev. B* **75**, 155111 (2007).
- [82] S. M. Abuelenin, *Physica A: Statistical Mechanics and its Applications* **492**, 564 (2018).
- [83] A. A. Abul-Magd and A. Y. Abul-Magd, *Physica A: Statistical Mechanics and its Applications* **396**, 185 (2014).
- [84] C. Jisha and R. Prakash, *Europhysics Letters* **146**, 11001 (2024).
- [85] M. Suezen [10.5281/zenodo.17912257](https://zenodo.org/record/17912257) (2025).
- [86] M. Suezen [10.5281/zenodo.18171032](https://zenodo.org/record/18171032) (2026).